Sixth International Conference on Durability of Concrete Structures **Paper Number KN08**
18 - 20 July 2018
University of Leeds, Leeds, West Yorkshire, LS2 9JT, United Kingdom

Mesoscopic model of drying shrinkage and its application into control of shrinkage cracking

T. Nawa
Hokkaido University, Sapporo, Japan

ABSTRACT

Concrete shrinks when it is subjected to drying, whenever its surfaces are exposed to air of a low relative humidity. In such a situation, cracking is to be expected, since there are various kinds of restraint that prevent concrete from contracting freely. Unless the ambient relative humidity is kept at close to 100%, such shrinkage cracking presents a critical problem in concrete construction, in particular for thin, flat structures such as walls and slabs in buildings, highway pavements, and bridge decks. This paper review the state of art of theory drying shrinkage from focus on the fact that microstructure in cement paste matrix consists of slit like pores as well as cylindrical shape pores. According to this fact, a new mesoscopic model of drying shrinkage is proposed. Our model can reproduce the experimental hysteresis loop of drying shrinkage for hardened cement paste, and reveals that drying shrinkage is closely related to the interaction potential between C-S-H nano-scale particles in cement systems. Meanwhile controlling cracking is essentially accomplished by reducing drying shrinkage. This paper also describes the efficiency of shrinkage reducing admixtures (SRAs) in controlling the restrained shrinkage cracking of concrete based on the mechanism of drying shrinkage.

Keywords: Hardened cement paste, Mesoscopic model, Drying shrinkage, Slit-like pore, C-S-H, Shrinkage reducing admixture.

1.0 INTRODUCTION

Drying shrinkage occurs in hardened concrete as a result of water movement. The major factors influencing drying shrinkage of concrete are the relative humidity, aggregate type and content, water content and the water-to-cement ratio (w/c). When concrete is wetted, it expands. This expansion phenomenon is referred to as swelling. Swelling is small compared with shrinkage in ordinary concrete and only when the relative humidity is maintained above 94% (Loman, 1940). The change in the moisture content of cement paste makes concrete shrink or swell. To better understand the influence of moisture content on drying shrinkage, one should consider the microstructure of the cement paste. The reaction of cement and water generates mainly a calcium silicate hydrate (C-S-H) gel with water-filled space. The size of the pores formed in the water-filled space is ranged form large capillary pores to smaller spaces in the C-S-H gel that are filled with adsorbed water.

The volume changes due to drying and wetting produces visible and invisible cracking in concrete under restraint conditions. Such cracks may influence the durability of reinforced concrete, e.g. the spoiling the surfaces of concrete structures, in particular for thin, flat structures such as walls and slabs in buildings, highway pavements, and bridge

Thus, the concrete shrinkage has been investigated for many decades, and multitude of mechanism has been proposed for shrinkage of hardened cement paste: capillary tension (Powers, 1965; Feldman, 1968), disjoining pressure (Bažant, 1972; Wittmann, 1973; Maruyama, 2010), surface energy (Wittmann, 1968; Feldman and Sereda, 1964), and changes in the basal spacing of layered hydrates (Feldman and Sereda, 1968, Beaudoin *et al*., 2010; Gutteridge and Parrott, 1976).

Deposit extensive studies of drying shrinkage, no complete theory has been proposed until now, combined theory of several mechanisms depending on the humidity have been commonly adopted to explain all of the observations (Wittmann, 2009). As drying occurs, disjoining pressure removes adsorbed water from the pores and capillary tensions form a meniscus that exerts stresses on the C-S-H skeleton causing the hardened cement paste to shrink. Thus capillary pressure becomes important when pore fills up water continuously, whereas disjoining pressure is prior to it at low degree of saturation.

Several researchers proposed the models to connect between measured sorption isotherms with pore structure to make clear the associated properties of porous materials. These models link the evaporation and condensation of water at a

given Relative Humidity (RH) with the width and connectedness of the pores over a range of scales (Baroghel-Bouny, 2007; Ranaivomanana *et al*., 2011; Bonnaud *et al*., 2012; Bonnaud *et al*., 2013).

Firstly models for mesoporous materials are typically extensions of the Kelvin-Laplace theory. But cement paste has a multiscale pore structure leads to hysteresis over the whole range of RH from 0% to 100%. For cement paste, the water in C-S-H gels plays the key role in drying shrinkage behavior as well as clay materials, but in contrast to Vycor glass, the volume at a given RH is smaller during wetting than during drying. Thus a self-consistent model of both sorption and drying shrinkage that can explain the hysteresis and the difference between cement paste and other mesoporous materials is requested.

This paper first reviews the previous studies on water-vapour sorption isotherm and drying shrinkage, and consequently proposes a new mesoscopic model of shrinkage accounting into the microstructure of C-S-H gel. Next the new model is applied into the methodology for reducing the shrinkage to control drying cracking; that is, new concept to reduce drying shrinkage is proposed and confirmed the validity of our mesoscopic shrinkage model by our past experiment data of shrinkage reducing admixture.

2.0 PREVIOUS STUDIES ON WATER SORPTION ISOTHERM: CLASSIFICATION OF WATER IN HARDENED CEMENT PASTE

Hysteresis of sorption isotherm associated with absorbate condensation and evaporation in mesoporous materials such as cement paste (see in Fig. 1) has been the subject of enormous interest for several decades because of its use in the characterization of pore size distribution. The hysteresis loop indicates the insight into the structure of the pore array that cannot be deduced from either the adsorption boundary or the desorption boundary of the hysteresis loop in sorption isotherm.

Using the Kelvin equation, which describes the thermodynamic equilibrium of a curved gas–liquid interface, Cohan proposed that irreversibility of capillary condensation is due to the different geometries of the gas–liquid interface upon adsorption and desorption (Cohan, 1938). However, adsorption in mesoporous materials such as hardened cement paste takes place in two distinct steps. During adsorption at low pressure, the fluid becomes adsorbed on the pore walls so that a multilayered liquid-like film grows. The thermodynamic properties of such a film are determined by the attractive interactions with the pore walls and surface tension γ_{GL} at the gas-liquid interface. At a certain thickness t_c, the surface tension makes the film thermodynamically unstable and capillary condensation takes place so that the pore is filled with a liquid-like adsorbate. This corresponds to a certain pressure P_c, which strongly depends on the pore size. In the reverse process, when desorption takes place from a liquid-filled pore, the system passes the P_c point and equilibrium capillary evaporation occurs at the pressure P_e, at which the grand potential of a filled pore equals the grand potential of the pore with a liquid film of a certain thickness. The difference between P_e and P_c is the most common origin of hysteresis observed in adsorption isotherms in mesoporous materials.

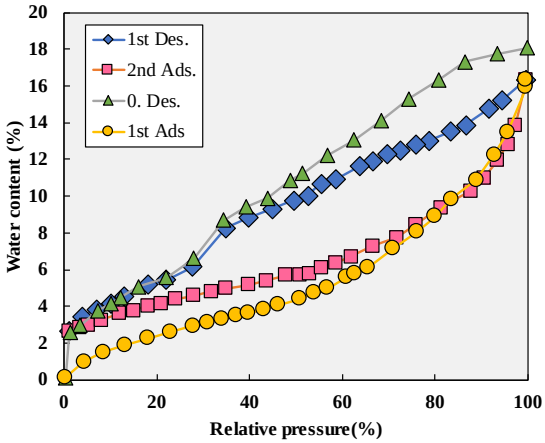

Fig.1. Sorption Isotherms for hardened cement paste: W/C = 0.40 (Setzer, 2008)

Describing capillary condensation and evaporation using the Kelvin equation has a fail to ignore the formation of a film adsorbed at the pore wall surface prior to capillary condensation. For large pores, such approximation by omitting an adsorbed film is reasonable, but it becomes inaccurate for micro- and meso-pores of which diameters are the same order of magnitude as the thickness of the adsorbed film. In 1974 Saam and Cole developed a theory of the thermodynamics and dynamics of thin films adsorbed in porous materials (Cole and Saam, 1974). In 1976 Derjaguin and Churaev also proposed a thermodynamic model which allows describing both the formation of an adsorbed film at the pore surface and capillary condensation–evaporation (Derjaguin and Churaev, 1976). In this model, adsorption and pore filling are described as the growth of an adsorbed film whose instability at a given pressure provokes capillary condensation. Due to the fact that the limit of stability of the film differs from the pressure at which the adsorbed phase is in phase equilibrium with the confined liquid separated from the gas external phase through a hemispherical meniscus, the model proposed by Derjaguin and Churaev allows describing the hysteretic behaviour of capillary condensation and evaporation. In this model, which is derived in the frame of the Gibbs dividing surface theory, the grand free energy Ω of a system comprises a cylindrical

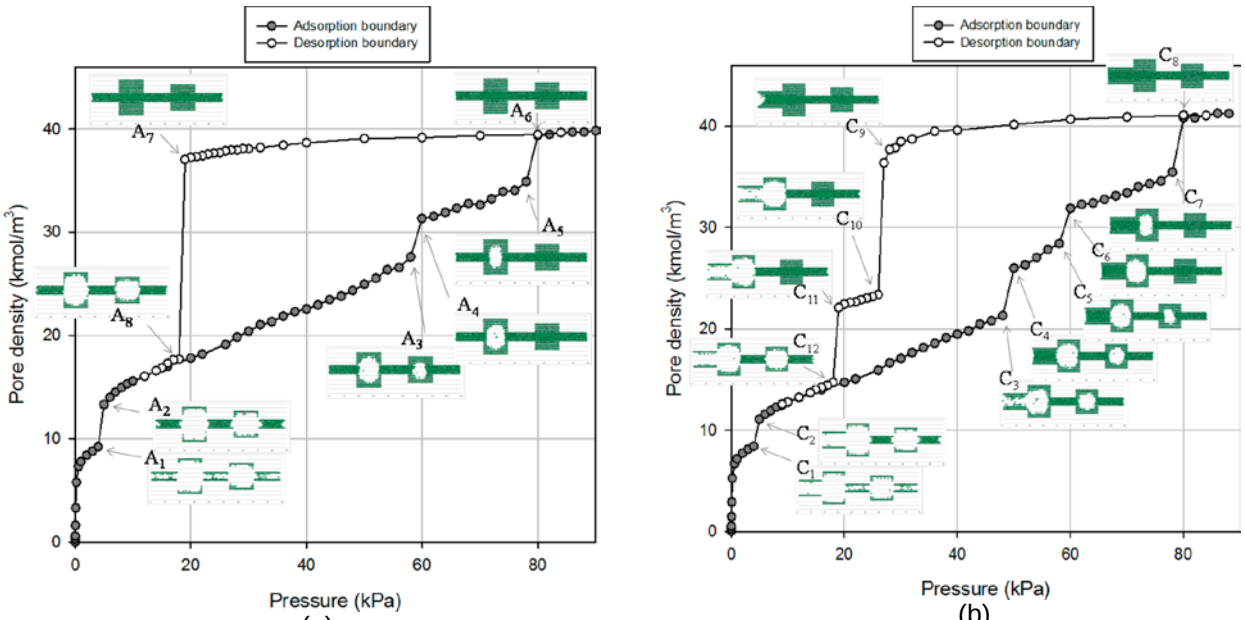

Fig.2. Adsorption−desorption isotherms of argon using Grand Canonical Monte Carlo simulation at 87 K in mesopore arrays consisting of two cavities and three necks: (a) This array has all three necks smaller than the critical width, *H*c; (b) This array has two necks smaller than the critical width *H*c and the neck connecting the large cavity to the gas surroundings greater than *H*c (Klomkliang *et al*., 2015)

pore of length L and radius R and the film of a thickness t adsorbed at the pore surface is written as (Derjaguin and Churaev, 1976, Coasne *et al*., 2013):

$$\Omega = P_G V_G \quad P_S V_S \quad P_L V_L + \gamma_{SL} A_{SL} + \gamma_{LG} A_{LG} + A_{LG} W(t) \tag{1}$$

where P_G, P_L, P_S, $V_G = \pi L(R- t)^2$, $V_L = \pi L(R^2- (R -t)^2)$, V_S are the pressure and volume of the gas, adsorbed, and solid phases, respectively. γ_{LG}, γ_{SL} and $A_{LG} = 2\pi L(R-t)$, $A_{SL} = 2\pi LR$ are the gas-adsorbed phase and solid-adsorbed phase surface tensions and surface areas, respectively.

The interface potential $W(t)$ in Eq.(1) allows describing adsorption at the surface of the material as it accounts for the interaction between the adsorbate molecule and solid surface. $W(t)$ is related to the disjoining pressure $\Pi(t)$ which is often invoked to describe adsorption phenomena and deformation of porous materials (Coasne *et al*., 2013):

$$\Pi(t) = \frac{dW(t)}{t} \tag{2}$$

However, the theoretical predictions from the models mentioned above is often different from experimental data since theories are usually developed using regular pores of a simple geometry which depart from real materials. In contrast, molecular simulations allow studying the thermodynamics and dynamics of fluids confined in more realistic and complex pores with considering several topological or morphological parameters such as constrictions, interconnectivity, and surface defects. Molecular simulations are thus an available tool to link theories and experimental results obtained for real mesoporous materials.

Figure 2 shows the hysteresis loops for argon isotherms using Grand Canonical Monte Carlo simulation at 87 K in mesopore arrays consisting of two cavities and three necks (Klomkliang *et al*., 2015). For the adsorption branch in Fig.2 (a), of which pore array has all three necks smaller than the critical width, H_c, as pressure is increased from an empty pore, molecular layering occurs on the pore walls, and the thickness of the adsorbed layer increases with pressure up to Point A_1, which is the condensation pressure of the three necks (equal in size). At this point the necks are filled with adsorbate (Point A_2), and it is worth noting that this condensation is that of open ended pores. As pressure is further increased from Point A_2 the adsorbed layers in the two cavities become thicker, and at Point A_3−A_4 condensation occurs in the small cavity, followed by a further increase in the thickness of the adsorbed layer in the large cavity, and finally condensation occurs in this cavity at Point A_5−A_6.

On the other hand, the desorption branch from a completely filled pore, the condensed fluid in the two cavities is stretched to Point A_7, at which evaporation from the two cavities occurs via the cavitation mechanism. In previous studies, pore blocking has been recognized as a possible emptying mechanism in pores such as ink-bottle pore with disordered shape and connectivity, cavitation has only been proposed and identified as another mechanism recently. The emergency of pore blocking or cavitation depends on the relative stability of the liquid confined in the constriction and the liquid confined in the cavity.

Starting with a completely filled pore, the liquid trapped in a cavity isolated from the gas phase through a filled constriction experiences a depression as the pressure decreases. Pore blocking is observed if the liquid in the cavity can resist such a depression until the liquid in the constriction evaporates. In that case, the desorption of the liquid located in the constriction spontaneously triggers the evaporation of the liquid cavity (the latter being already at a pressure below its equilibrium pressure). On the other hand, cavitation is observed if the liquid in the cavity cannot resist the depression until the liquid in the constriction evaporates. In that case, the desorption of the liquid located in the constricted pore occurs through the spontaneous nucleation of a gas bubble while the constriction remains filled by the liquid. These two desorption mechanisms, cavitation and pore blocking, are illustrated in the inset of Fig. 2.

The information about the width (H_c) of neck pore can be determined from the desorption pressure. Also the large cavity width H can be estimated from the condensation pressure by assuming that it corresponds to the evaporation pressure of a cylindrical pore having the same diameter. It should be emphasized that in the case of very small pores, the cavitation pressure depends on the cavity size, the desorption mechanism in disordered pores is governed by H_c/H instead of H_c.

The evaporation mechanism in constricted pores depends on the size of the constrictions in the pores. If the desorption can occur through pore blocking, the cavities will be empty when the constrictions that isolate them from the external bulk phase empty. On the other hand, if the desorption can occur through cavitation, the nucleation of a gas bubble within the cavity and consequently the cavities will be empty while the constrictions remain filled by the liquid. Furthermore, there is the difference of pressure to empty the cavities. Pore blocking occurs at a pressure determined by the size of the constrictions, while cavitation occurs at a pressure determined by the spontaneous nucleation of a gas bubble that mainly depends on the bulk properties of the fluid and temperature.

Indeed, when one neck pore shown in Fig. 2(b) is changed to one larger than the critical width, changing one neck shown in Fig. 2(b) to a large pore with larger width than the critical width H_c, the adsorbate in the large cavity empties first along the vertical segment C_9-C_{10} by a pore blocking mechanism, because it is connected to the gas through the large neck pore whose width is greater than H_c. On further reduction of cavitation of adsorbate takes place in the small cavity at C_{11}, which empties along the segment C_{11}-C_{12}.

Comparing the isotherm for matured cement paste (Roper, 1966, See Fig. 3) with the results Grand Canonical Monte Carlo simulation as shown in Fig. 2, we can divide water in hardened cement paste into four categories based on its local environment within the microstructure: Interlayer water, gel water, capillary water, and surface-adsorbed water.

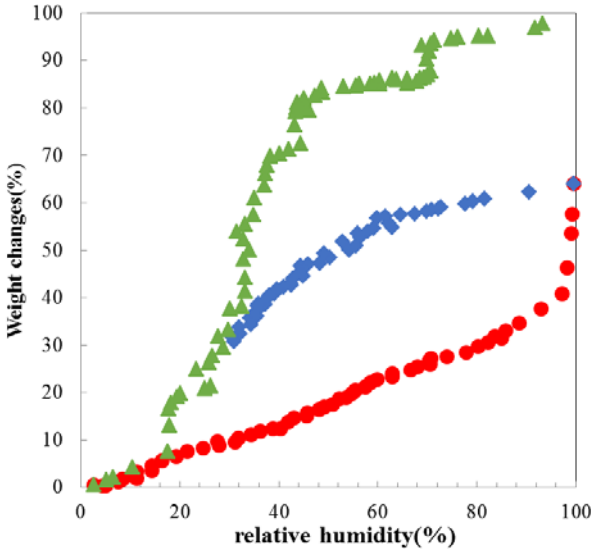

Fig.3. Relationship between relative vapor pressure and weight change (Roper, 1966)

Interlayer water in spaces with width of 2nm or less is bound strongly and is removed only at low RH. Traditionally, interlayer water is defined as residing between the silicate-rich layers of solid C-S-H integral to the structure of the solid. At that situation the water is in contact with rough surfaces built from silicate tetrahedra with nonhydroxylated dangling oxygen atoms. Furthermore, Jennings reported that substantial collapse and swelling of the interlayer space occur when water is removed and reinserted, respectively (Jennings, 2008). Thus it implies that the insertion of water into the interlayer space confers a mechanical disjoining effect.

Gel pores have also been defined as pores within the C-S-H gel. The gel pores has widths between approximately 2 and 10 nm. According to Aono *et al*. the structure of C-S-H varies with drying, gel pore changes greatly when compared before and after drying (Aono, *et al*., 2007).

Water in capillary pores with width greater than 10 nm are responsible for the hysteresis between drying and rewetting above 85%RH (Jennings, 2008; Jennings, 2004). NMR experiments (Muller, 2013) show that 85% RH is a relevant threshold value for the capillary pores to be empty. Since capillary pores is difficult to be filled up unless the sample is immersed; hence, pores of greater than 100 nm can be considered devoid of condensed water and simply lined with a thin shell of adsorbed water.

Surface-adsorbed water in empty pores is defined as the water present in gel and capillary pores after pores are empty of bulk water, present as a thin adsorbed layer on the walls. This adsorbed water is influential in determining shrinkage because it affects the surface energy of the solid-pore interface.

3.0 PREVIOUS MODEL ON ADSORPTION STRESS AND SHRINKAGE

Several researchers extend to mesoporous materials a simple yet instructive thermodynamic model of the adsorption stress. The proposed model relates the stress exerted by the adsorbed phase on the adsorbent framework, with the adsorption isotherm. From the thermodynamic standpoint, the adsorption stress σ_s can be quantified by the derivative of the grand thermodynamic potential Ω of the adsorbed phase with respect to the pore volume V at a given temperature T and adsorbate chemical potential μ (Gor and Neimark, 2010; Gor *et al*., 2017).

$$\sigma_s = \left(\partial\, \Omega / \partial V\right)_{\mu,T} \tag{3}$$

Hence volume changes with a slit-like pore with two immobile plates can be written as (Schiller *et al*., 2008):

$$\frac{\Delta V}{V} = \frac{\sigma_s}{K_{\text{eff}}} \tag{4}$$

where K_{eff} is the effective elastic modulus of the hardened cement paste, which responds to interior tensions produced by pores.

The thermodynamic approach overviewed above gives adsorption stress can describe deformation of mesoporous solids such as MCM-41 and Vycor glass in the course of adsorption-desorption hysteretic cycles as shown in Fig. 4 although it leaves the elastic modulus M in Eq. (4) as a fitting parameter (Gor *et al*., 2017).

However, cement paste exhibits completely opposite hysteresis (see Fig. 5). That is, swelling during the adsorption process is smaller than shrinkage during the desorption process over the whole range of RH from 0% to 100%.

Pinson *et al*. predicted the swelling and shrinkage behaviour of hardened cement paste using continuum model of deformation induced by RH change. Their model based on poromechanics can accounts separately for the three categories of pressure from gel and capillary water, interlayer water and surface water (Pinson *et al*., 2015). The results indicated that the hysteresis in swelling and

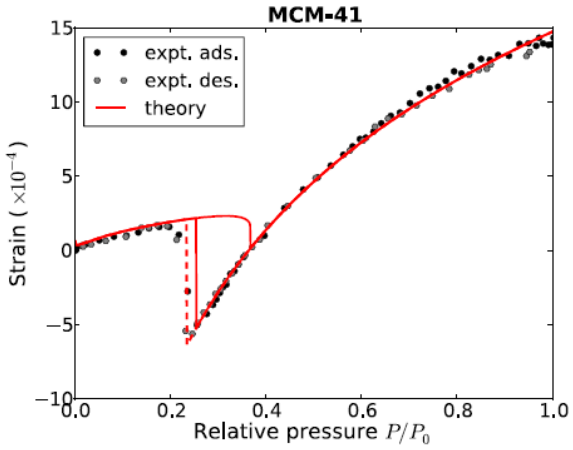

Fig. 4. Adsorption-induced strain isotherm for n-pentane adsorption on MCM-41 silica. Circles represent the experimentally measured strain from in situ SAXS (Gor *et al*., 2013) and lines represent theoretical calculations (Gor *et al*., 2017).

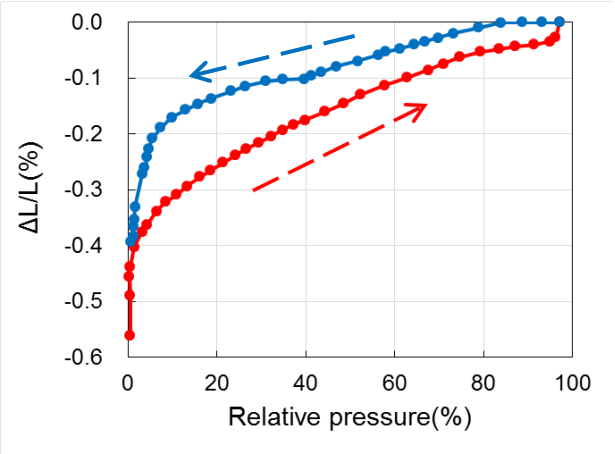

Fig. 5. Shrinkage for Portland cement paste vs. Relative humidity (Feldman, 1968).

shrinkage due to capillary pressure shows opposite direction, while the swelling effect of interlayer water plays a major role in hysteresis in swelling and shrinking behaviour. Feldman and Sereda pointed out that the reversal phenomenon does not occur when rewetting is initiated before drying below 25% RH (Feldman and Sereda, 1966). This indicates that the desorption and evaporation of interlayer water and some gel water, which holds water even at 25% RH, is the cause of hysteresis in swelling and shrinkage of hardened cement paste.

However, they derivate the swelling and shrinkage due to the change in quantity of interlayer water based on a simple model that the strain is linearly proportional to the quantity of the interlayer water. This is empirical model and does not make clear the detailed action mechanism in which shrinkage occurs. Thus a self-consistent model of drying shrinkage that captures the hysteresis and explains the difference between cement paste and other mesoporous materials, like Vycor, is still lacking.

4.0 NEW MESOSCOPIC MODEL OF DRYING SHRINKAGE

In order to construct a self-consistent model of drying shrinkage, it is necessary to know the microstructure of hardened cement paste, in particular, the structure of C-S-H which strongly affects drying shrinkage of cement paste.

Recently, Jennings proposed a new hybrid model of C-S-H, which treats C-S-H as a gelled colloid and a granular material as shown in Fig 6 (Jennings, 2008). In his model the LD (low density) C-S-H gel is composed of aggregates of lamellar particles called globules. The globule pack together as colloids or grains of solid, and aggregates of globule fill space with specific packing densities. Notice that the globules have one set of properties, but their larger scale packed arrangement has another set of properties.

He also indicated that in the cement paste there exist small gel pore (SGP), large gel pore (LGP) and intraglobular pore (IGP) as well as capillary pores which are the voids which were originally filled in the hydrate by the space occupied by the kneading water. Form the Fig. 6 it seems that capillary pore and LGP may be not like slit-like pore, but rather as cylindrical pore. In contract, both SGP and IGP are consists of slit-like pores. Furthermore, Jennings also insisted irreversible drying shrinkage is due to rearrangement of packing of the globules often with the effect of reducing the volume of gel pores in the 5 - 12 nm range (Jennings, 2007).

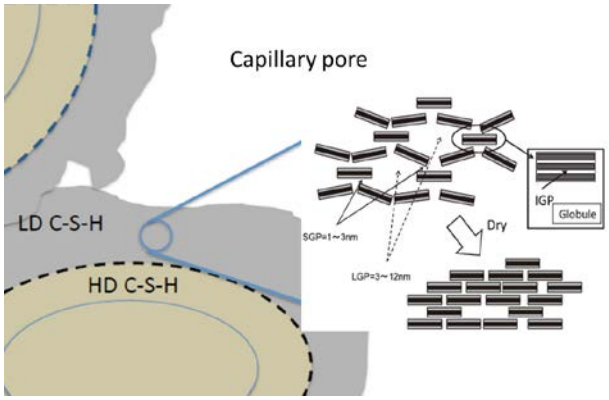

Fig. 6. Schematic of C-S-H gel (Jennings, 2008)

From these results of past studies, it is realistic that C-S-H particles are combined not by the chemical bond, but physical bond. In other words, it can be considered that C-S-H has slit type pores, which is not fixed and can be moved. In fact, the slit-type pores exhibit hysteresis curves similar to those of the cylindrical pores when the distance between the plates is fixed. This leads to the hypothesis that two parallel plates that configure slit-like pores can move freely each other. Here we shall consider is the more realistic slit-like pore, which consist of two parallel plates and the distance between two plates is variable (see Fig. 7).

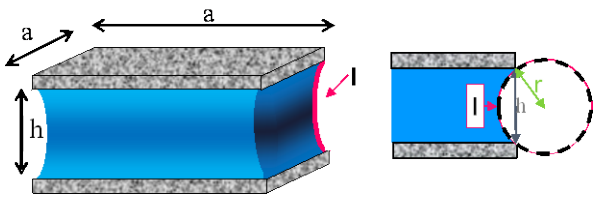

Fig. 7. Schematic of slit-like pore with mobile parallel plates

The interplanar distance without humidity change can be determined by the minimum value of the grand thermodynamic potential Ω of the adsorbed phase with respect to the pore width h at a given temperature and absorbate chemical potential. This condition can be given by the following equation:

$$\left(\partial \Omega/\partial h\right)_{\mu,T} = 0 \tag{5}$$

In this system the liquid-gas interface is present in the four sides of the slit-like pore since the pore is always completely filled with water. It should be noted that the free energy due to disjoining pressure become a function of two parameters of the width h and decay length λ. Approximating the surface area of liquid-gas interface with $2ah$, the grand canonical potential Ω of a slit-like pore with two mobile plates can be rewritten as:

$$\frac{\Omega(h,\lambda)}{a^2} = 2\gamma_{SL} + 4l(p)(l/a)\gamma_{LG} - \frac{h}{V_m}RT\ln(p/p_0) + \frac{\omega(h,\lambda)}{a^2} \tag{6}$$

where a is the surface area for plate consists of slit-like pore, V_m is the molar volume of water, R is the gas constant, T is absolute temperature and P/P_0 is the relative vapor pressure and $l(p)$ is the length of meniscus at the liquid-gas interface. $\omega(h,\lambda)$ is the disjoining pressure potential.

Several researchers have been proposed the different type formulas to represent $\omega(h,\lambda)$. In this study, the author adopts the following two-parametric expression for slit-like pore proposed by Marceja and Radic (Marceja and Radic, 1976):

$$\frac{\omega(h,\lambda)}{a^2} = \lambda\Pi_0\frac{\exp(h/\lambda)+1}{2\sinh(h/\lambda)} \tag{7}$$

where λ is the decay length, a is the surface area for plate consists of slit-like pore and Π_0 (N/m^2) is disjoining pressure. The unknown parameter for $\omega(h,\lambda)$ can be obtained from the experimental data about the thickness of water film on cementitious material surface.

Badmann *et al*. quantified the statistical thickness of adsorbed water film on two nonporous C_2S and C_3S at 293°K (Badmann *et al*., 1981). The thickness of water film h is determined from the equation, and is represented as a function of vapour pressure P/P_0. On the basis of our fitting we obtain the values of the parameters to be used for modelling water adsorption on hardened cement paste surface: $\Pi_0 = 20\times10^6 N/m^2$, $\lambda = 1nm$.

Based on the thermodynamics, the expansion of slit-like pore due to an increase of the relative humidity from P/P_0 to $(P+\Delta P)/P_0$ requires the work $W(h)$ that put the water of increased volume ΔV into the slit-like pore. This work should be done against the interaction force, so-called disjoining pressure acting between the two parallel flat plates, which is given by the following equation:

$$W(h) = \int_{h}^{h+\Delta h} \frac{\partial\, \omega(h,\lambda)}{\partial\, h} dh \qquad (8)$$

where Δh is the increment of width of slit-like pore due to change in the relative humidity from p/p_0 to $(P+\Delta P)/P_0$

It should be noted that, in the grand canonical potential of the state at relative humidity of $(P+\Delta P)/P_0$ is equal to the sum of grand canonical potential of the state at relative humidity of P/P_0 and the excess work expressed in Eq. (8). According to this procedure, we can calculate the pressure increment ΔP corresponding to the increase of the width of slit-like pore.

For the shrinkage in the desorption process, we should consider the work to extract the water of ΔV from the slit-like pore, and the canonical potential of the state at relative humidity of $(P-\Delta P)/P_0$ is equal to that to subtract the excess work ΔW from the grand canonical potential of the state at relative humidity of p/p_0. Further, the volume changes are calculated using Eqs. (3) and (4).

On the other hand, the dry shrinkage of the cylindrical pores is estimated using the model proposed by Schiller *et al*. (Schiller *et al*. 2008).

Figure 8 shows the obtained theoretical swelling-shrinkage isotherms assuming that (a) all pore are slit-like and (b) all pores are cylindrical by using the experimental data of water-vapour sorption isotherms and swelling-shrinkage isotherms for cement paste published by Feldman and Sereda (Feldman and Sereda, 1968) of which sample is dried by degassing at 80°C. It can be seen that as compared with experimental data, the hysteresis in the shrinkage of cylindrical pores shows the opposite direction and underestimates the shrinkage. On the other hand, the shrinkage hysteresis of slit-like pore shows the same direction, but overestimates.

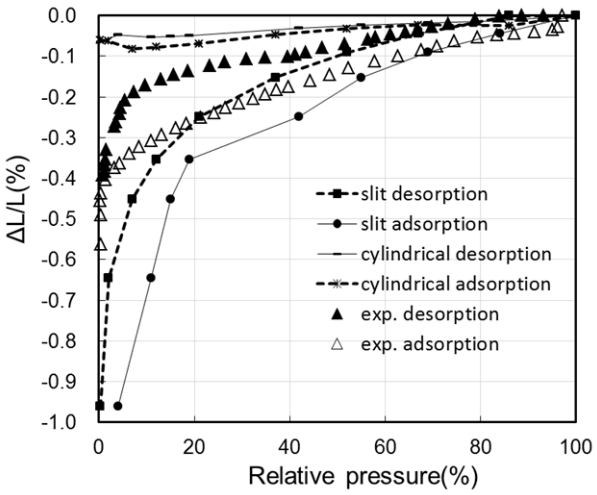

Fig.8. Shrinkage for cylindrical pore and slit-like pore predicted by our model as compared with the experimental data (Feldman, 1968)

From the previous discussion on the microstructure of C-S-H, we assume that capillary pore and LGP consist of cylindrical pores, while SGP and IGP consist of slit-like pores, and calculate the deformation induced by humidity change in cement paste. The results is illustrated in Fig. 9 along with the experimental data (Feldman and Sereda, 1968). It can be seen that our model successfully reproduces the magnitude and general shape of the hysteresis in the reversible drying strain. Since our model can apply the other porous materials, we can construct a self-consistent model of drying shrinkage that captures the hysteresis and explains the difference between cement paste and other mesoporous materials. In addition, it can be seen that the changes in interlayer and small gel water may translate or upscale to macroscopic volume changes.

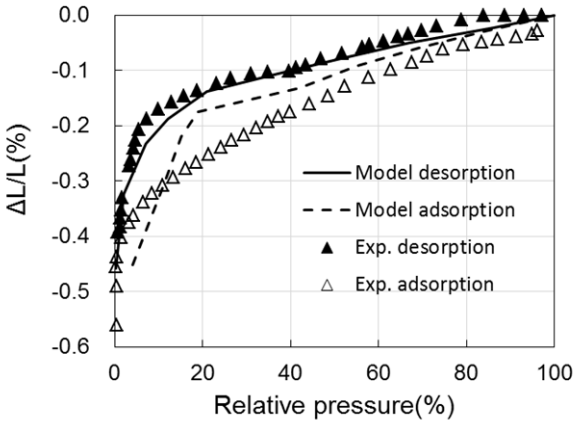

Fig.9. Mesoscopic model prediction and experimental data (Feldman, 1968) for shrinkage of cement paste accounted into both slit-like pore and cylindrical pore

5.0 APPLICATION OF MESOSCOPIC MODEL OF SHRINKAGE INTO CONTROL OF SHRINKAGE CRACKING

There are two most common methods of reducing the potential for cracking in early ages of concrete (Weiss and Berke, 2002). The first approach is to reduce the magnitude of shrinkage, namely the intensity of stress in the material, while the second method is to reduce the rate of shrinkage, namely the rate of stress development, providing time to allow the cracking resistance to increase. Concrete containing shrinkage reducing admixture (SRA) generally shows a lower rate of shrinkage and a reduction in the overall magnitude of shrinkage. Thus, it is possible that the utilization of SRA presents a novel approach to minimizing drying shrinkage.

SRA that serves to reduce the surface tension of the pore fluid in concrete, was first developed in the 1980's in Japan (Sato *et al*., 1983; Tomita *et al*., 1986). For the last few decades, several different SRAs have appeared on the market. The amount of shrinkage reduction due to SRA depends on its concentration, and the amount of reduction in drying shrinkage appears to be relatively independent of the w/c when the aggregate volume and the type are the same. The presence or absence of SRA does not significantly change the amount of water lost, however, it is a significant factor in the length change (Weiss and Berke, 2002).

Most researchers indicate that the use of an SRA, typically 2% - 5% by weight of water, results in a substantial reduction in overall shrinkage. A study of restrained shrinkage shows an increase in the resistance to early age cracking when an SRA is used. Experiments performed using slabs restrained at both the base and the ends indicate that the use of SRA can substantially increase the distance between cracks (Shah *et al*., 1997). This is significant, in that it may provide a justification for permitting larger joint spacing in concrete containing SRA. SRA also contributes to a reduction in autogenous shrinkage in high performance low w/c concretes (Bentz and Jensen*,* 2004*;* Weiss *et al*., 1999) and improves the resistance of concrete to plastic shrinkage cracking (Lura *et al*., 2007). Therefore, SRA has proved to be extremely beneficial in reducing the risk of shrinkage cracking in concrete elements.

The influence from SRA has been explained by the reduction in the surface tension of a pore fluid. The surface tension of the pore fluid affects the capillary tension. Thus, the shrinkage reducing mechanism of SRA has been mainly explained by the reduction of capillary tension in surface tension of a pore fluid. Based on our mesoscopic model, the mechanism of conventional SRA can be interpreted by the decrease of second terms in Eq. (6).

However, since the change of free energy is smaller, it is too difficult to be explained theoretically the effect of SRA from view point of surface tension. Indeed Tomita points out that the relation between drying shrinkage and the specific surface tension of the SRA varies depending on the type of SRA (Tomita, 1992). The author attempted to verify the effect of w/c on autogenous shrinkage, based on the changes in capillary pressure with the w/c. It can be seen that the capillary pressure theory is not capable of explaining the influence of the surface tension on autogenous shrinkage. This implies that some other driving force, such as disjoining pressure, is contributing to the effect of SRA.

Conventionally, it is thought that the capillary tension is dominant in dry shrinkage at high relative humidity, but based on our mesoscopic model it suggests theoretically that disjoining pressure is superior even at high relative humidity. This also coincides with the result of Fig.6 which shows that the drying shrinkage of the slit-like pores dominating the disjoining pressure dominates the total drying shrinkage of hardened cement paste. These discussion leads to a conclusion that one of methodologies to control shrinkage cracking of concrete is the control of disjoining pressure in hardened cement paste.

Ferraris and Wittmann introduced that disjoining pressure is essentially the sum of a series of attractive forces such as the Van der Waals force and repulsive forces such as a double-layer repulsion due to surface charge and the structural force of water molecules on pore wall (Ferraris and Wittmann, 1987). Double-layer repulsion is strongly affected by the chemical composition of the pore solution. These forces act not only on the surfaces of cement particles but also on the surfaces of the finer particles of hydrates such as C-S-H gel. The ionic concentrations of the pore solution vary according to the w/c. As the w/c decreases, the ionic concentration gradually increases and then the double-layer repulsion decreases. At this moment, the fine particles in the C-S-H gel flocculate, so that the total C-S-H gel shrinks macroscopically.

It is well known that the steric interaction between two adsorbed polymer layers absorbed on the pore plates consist of slit-like pore can also influence the disjoining pressure. Indeed, as shown in Fig. 10, the SRA that we used this time consists of a polycarboxylate-type polymer with a larger number of hydrophobic groups that is capable of strongly adsorbing onto cement particles (hereinafter referred to as NSR-1) with a surface tension similar to or slightly lower than water, and shows a higher drying shrinkage-reducing effect than the conventional SRAs that serve the lower surface tension of a pore solution in concrete (Masanaga *et al*., 2006).

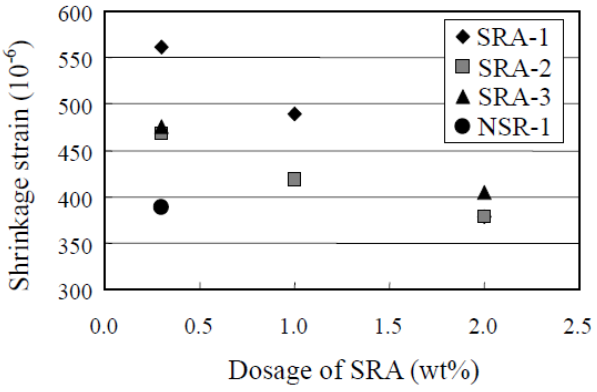

Fig. 10. Relation between dosage of SRA and shrinkage strain at 28 days: SRA-1, SRA-2 and SRA-3 are commercial SRAs of which component is poly-oxyalkylenegrycol, low-molecular-weight alcohols-alkylene oxide adduct and polyoxyalkylenegrycol alkyl ether, respectively

From the results of Fig. 10, it is confirmed that the water in IGP and SGP plays the important role in the swelling and shrinkage in cement paste. Further, the result also shows that the disjoining pressure between the surfaces of globule in C-S-H gel is the main driving force of drying shrinkage. This fact implies the possibility of development of new SRA which can control the disjoining pressure in C-S-H gel by the other way.

6.0 CONCLUSIONS

This paper has first reviewed the development of theoretical mesoscopic approach for sorption isotherm and shrinkage of porous materials such as cement paste. Previous studies on sorption isotherms indicates that there are four different water in the interlayer space, gel pore, and capillary pores, and adsorbed water on the pore wall. The review also indicates that for the previous shrinkage model of the other porous materials cannot reproduce the shrinkage of hardened cement paste and a continuum model can be consistent with measurement data using semi-empirical fitting parameters, but they does not make clear the driving force and mechanism of hysteresis.

The new mesoscopic shrinkage model is proposed without any adjustment based on the microstructure of C-S-H and interaction potential energy between globules and/or aggregates of globules which are the unite particles of C-S-H. The most important feature of our model is to introduce the slit-like pore which is formed between two globules. It does not bond chemically but only by physical intermolecular forces and consequently it can be moved by the interactions between the two globules. Our model successfully reproduces the magnitude and general shape of the hysteresis in the reversible drying strain. Our model also can explain the mechanism of reducing shrinkage admixture. This mechanism is confirmed by the experimental data using shrinkage reducing admixture without reducing surface tension.

References

Aono, Y. *et al*., 2007. Nano-structural Changes of C-S-H in Hardened Cement Paste during Drying at 50 ˚C, Journal of Advanced Concrete Technology, 5(3): 313-323

Bažant, Z.P., 1972. Thermodynamics of hindered adsorption and its implications for hardened cement paste and concrete. Cement and Concrete Research. 2: 1–16.

Badmann, R.*et al*., 1981. The Statistical Thickness and the Chemical Potential of Adsorbed Water Films. Journal of Colloid and interface Science, 82(2): 534-542.

Baroghel-Bouny, V., 2007. Water vapour sorption experiments on hardened cementitious materials part I: Essential tool for analysis of hygral behaviour and its relation to pore structure. Cement and Concrete Research, 37: 414.

Beaudoin, J. *et al*., 2010. Dimensional change and elastic behavior of layered silicates and Portland cement paste. Cem. Concr. Compos, 32: 25–33.

Bentz, D.P. and Jensen, O.M., 2004. Mitigation strategies for autogenous shrinkage cracking. Cement and Concrete Composites, 26 (6): 677–685.

Bonnaud, P.A. *et al*., 2012. Thermodynamics of water confined in porous calcium-silicate-hydrates. Langmuir, 28: 11422.

Bonnaud, P. A. *et al*., 2013. Effects of elevated temperature on the structure and properties of calciumsilicate-hydrate gels: The role of confined water. Soft Matter, 9: 6418.

Coasne, B. *et al*., 2013. Adsorption, intrusion and freezing in porous silica: the view from the nanoscale. Chem. Soc. Rev., 42: 4141—4171.

Cohan, L. H. 1938. Sorption Hysteresis and the Vapor Pressure of Concave Surfaces J. Am. Chem. Soc., 60 (2):433–435.

Cole, M, W., Saam, W. F., 1974. Excitation Spectrium and Thermodynamic Properties of Liquid Films in Cylinder Pores: Physical review letters, 32: 985

Derjaguin, B. V., Churaev, N. V., Polymolecular adsorption and capillary condensation in narrow slit pores: Journal of Colliod and Interface Science, 54: 157-175

Feldman, R.F., Sereda, P.J., 1964. Sorption of water on compacts of bottle-hydrated cement. II. Thermodynamic considerations and theory of volume change. J. Appl. Chem., 14: 93–104.

Feldman, R.F., 1968. Sorption and length-change scanning isotherms of methanol and water on hydrated portland cement. Fifth international symposium on the chemistry of cement, Tokyo, 53–66.

Feldman, R.F., Sereda, P.J., 1968, A model for hydrated Portland cement paste as deduced from sorption-length change and mechanical properties, Mater. Constr., 1 509–520.

Ferraris, C. F., Wittmann, F. H., 1987. Shrinkage mechanisms of hardened cement paste. Cement and Concrete Research, 17:453-464.

Gor, G. Y., Neimark, A. V., 2010. Adsorption-Induced Deformation of Mesoporous Solids. Langmuir, 26(16): 13021–13027.

Gor, G. Y. *et al*., 2013. Adsorption of n‑Pentane on Mesoporous Silica and Adsorbent Deformation Langmuir, 29: 8601−8608.

Gor, G. Y. *et al*., 2017. Adsorption-induced deformation of nanoporous materials—A review. Applied Physics Reviews, 4: 11303-11322.

Gutteridge, W.A., Parrott, L.J., 1976. A study of the changes in weight, length and interplanar spacing induced by drying and rewetting synthetic CSH (I). Cem. Concr. Res., 6: 357–366.

Jennings, H. M., 2004. Colloid model of CSH and implications to the problem of creep and shrinkage. Materiaux et constructions Materials and structures, 37: 59.

Jennings, H.M. *et al*., 2007. A multi-technique investigation of the nanoporosity of cement paste. Cem. Concr. Res. 37:329-336.

Jennings, H. M., 2008, Refinements to colloid model of C-S-H in cement: CM-II. Cement and Concrete Research, 38: 275.

Klomkliang, N. *et al*., 2015. Hysteresis Loop and Scanning Curves for Argon Adsorbed in Mesopore Arrays Composed of Two Cavities and Three Necks. J. Phys. Chem. C, 119: 9355−9363.

Loman, W. R, .1940. The theory of concrete creep, Proceeding ASTM 40:1082-1102.

Lura, P., *et al*., 2007. Influence of shrinkage reducing admixtures on development of plastic shrinkage cracks. ACI Materials Journal, 104 (2):187–194.

Masanaga,M, Yamamoto, T., Hirata, T., and Nawa, T., 2006. A New High Performance Drying Shrinkage-Reducing Admixture. V.M. Malhotra (Ed.), Superplasticizers and Other Chemical Admixtures in Concrete. Proceedings of the Seventh CANMET/ACI International Conference (ACI SP-239), Sorrento, Italy, 297-307.

Marcelja, S., Radic, N., 1976. Repulsion of interfaces due to boundary water, Chem. Phys. Lett., 42:129–130.

Muller, A. C. A. *et al*., 2013. Use of bench-top NMR to measure the density, composition and desorption isotherm of C-S-H in cement paste, Microporous Mesoporous Mater., 178:99.

Pinson, M.B. *et al*. 2015. Hysteresis from Multiscale Porosity: Modeling Water Sorption and Shrinkage in Cement Paste, Phys. Rev. Applied 3 (6) : 064009.

Powers, T. C., 1965. The mechanics of shrinkage and reversible creep of hardened cement paste, Cement and Concrete Association. International Conference on the structure of Concrete. London, 319–344.

Ranaivomanana, H. *et al*., 2011. Toward a better comprehension and modeling of hysteresis cycles in the water sorption–desorption process for cement based materials. Cement and Concrete Research, 41: 817.

Ravikovitch P. I., Neimark, A.V., 2006. Density functional theory model of adsorption deformation, Langmuir, 22: 10864.

Roper, H, 1966. Dimensional change and water sorption studies of cement paste. Special Report, Highway Research Board, 90: 74-83.

Sato, T. *et al*., 1983. Mechanism for reducing drying shrinkage of hardened cement by organic additives. CAJ Review, 37: 52–55.

Schiller, P. *et al*., 2008. Mesoscopic model of volume changes due to moisture variations in porous materials. Colloids and Surfaces A: Physicochem. Eng. Aspects 327:34–43

Setzer, M. J., 2008. The solid-liquid gel-system of hardened cement paste. Creep, Shrinkage and Durability Mechanics of Concrete and Concrete Structure, 1:237-243.

Shah, S.P. *et al*., 1997. Control of Cracking with Shrinkage-Reducing Admixtures. Journal of the Transportation Research Board, 1574: 25-36.

Tomita, R., 1992. A Study on the Mechanism of Drying Shrinkage Reduction through the Use of an organic Shrinkage Reduction Agent. Concrete Library, 19: 233-245

Tomita, R. *et al*., 1986. Properties of hardened concrete impregnated with cement shrinkage reducing agent. CAJ Review, 40:314–317.

Weiss, J. *et al*., 1999. The influence of a shrinkage reducing admixture on the early age shrinkage behavior of high performance concrete. Proceedings of International Symposium on Utilization of High Strength/High Performance Concrete, Sandefjord, Norway, 2: 1339–1350.

Weiss, W. J., and Berke, N.S., 2002. Admixtures for Reduction of Shrinkage and Cracking. Early Age Cracking in Cementitious Systems - State of the Art Report, ed. A. Bentur, RILEM

Wittmann, F.H., 1968. Surface tension skrinkage and strength of hardened cement paste. Mater. Constr., 1: 547–552.

Wittmann, F.H., 1973. Interaction of Hardened Cement Paste and Water, J. Am. Ceram. Soc., 56: 409–415.

Wittmann, F. H., 2009. Heresies on shrinkage and creep mechanisms. In: Tanabe *et al*. Ed., Proceedings of Creep, Shrinkage and Durability Mechanics of Concrete and Concrete Structures, London, Taylor and Francis Group, 3-10